

## FINITE ELEMENT ANALYSIS OF INJURIES IN SHOULDER

### BONES AND JOINTS: A REVIEW

A. CHENNAKESAVA REDDY

*Professor, Department of Mechanical Engineering, JNT University, Hyderabad, Telangana, India*

#### ABSTRACT

*Shoulder injuries are common vehicle accidents, sports activities fall during walking or running. The objectives of this were to identify different injuries occurring in the clavicle, the scapula and the proximal humeral head bones. The injuries were also identified in the gleno-humeral, the acromio-clavicular, the sterno-clavicular, and the scapulothoracic joints. The applications of finite element methods were also discussed for the fracture analysis of clavicle, scapula and for proximal humeral head, gleno-humeral, acromio-clavicular, sterno-clavicular, and scapulothoracic joints.*

**KEYWORDS:** *Clavicle, Scapula, Humerus, Gleno-Humeral Joint, Acromio-Clavicular Joint, Sterno-Clavicular, Scapulothoracic Joint, Finite Element Analysis*

**Received:** Jan 03, 2016; **Accepted:** Jan 12, 2016; **Published:** Feb 01, 2016; **Paper Id.:** IJBTRFEB20164

#### INTRODUCTION

The human shoulder comprises of clavicle, scapula, humerus bones and associated muscles, ligaments and tendons. These bones become unbalanced because the diameter of upper-arm ball is larger than that of shoulder socket. Consequently, it is the precinct of sprains, strains, dislocations, separations, tendinitis, bursitis, rotator cuffs tear, frozen shoulder, fractures and arthritis. To stay in a normal position, the shoulder must be secured by muscles, tendons and ligaments. The major shoulder injuries are rotator cuff injuries, labrum tears and fractures of the upper arm bone. Pinching of rotator cuff and swelling of tendon are results of repeated movement of arms over the head. These injuries are common in sports activities, for instance: pitching of baseball, heavy weight lifting, serving the tennis ball, bowling the cricket ball and swimming. The top of arm bone pinches the rotator cuff muscles against the top portion of shoulder blade due to repeated movement of arm over the head. This results in inflammation of the muscles. The tendon can tear if the movement is continued. When the labrum tears, the athlete senses pain in the shoulder. Upper arm fractures are consequences of a fall on an outstretched arm or from a direct blow. Upper arm fractures are familiar amongst older people.

This paper examines the variety of injuries that occur in clavicle, scapula and humerus and finite element approaches to analyze them. The joints associated with these three bones are further examined. Apart from these, glenoid cavity, acromion and coracoid processes are also discussed. Some prevention tips and simple remedies are as well addressed.

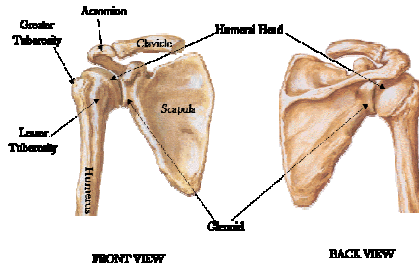


Figure 1: Shoulder

**SHOULDER BONES**

Figure 1 shows the bones representing the shoulder. The major bones are clavicle, scapula and humerus.

**Fracture Analysis of Clavicle**

The clavicle (figure 2) is the bone that runs horizontally between the top of sternum and scapula. The clavicle injuries are familiar in vehicle accidents and in cyclists when they fall. The clavicle is susceptible to fracture, particularly near the curves on account of its ‘S’ shape (figure 3a). The clavicle bone is the weakest link and tends to break due to force transmitted through the arm to the shoulder. Fractures are classified by their position along the bone and also by the amount of separation between the bone fragments. The clavicle injuries account for 4% to 10% of all adult fractures and 35% to 45% of fractures that occur in the shoulder girdle. However, fractures of the clavicle may not damage to nerves, blood vessels or lungs.



Figure 2: The Clavicle

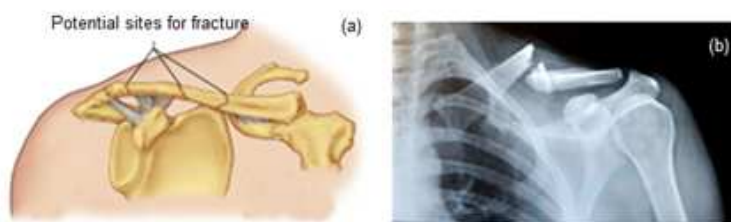


Figure 3: Fractures of Clavicle Bone

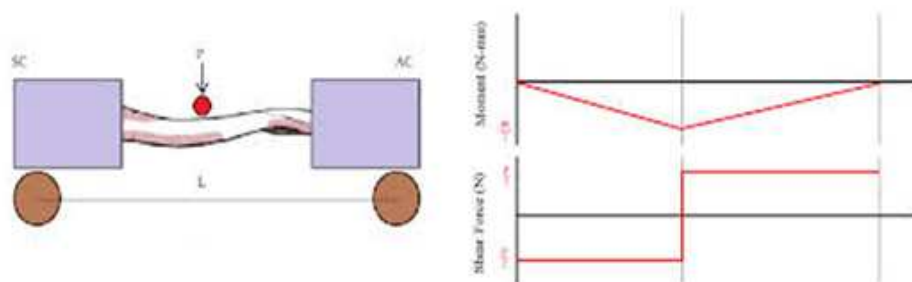
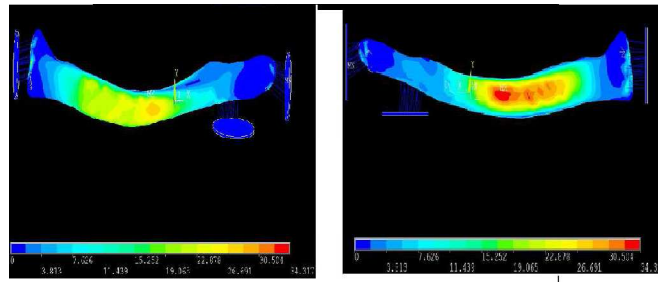


Figure 4: Three-Point Bending Test of Clavicle

Most of the researchers simulated the fracture behavior of the clavicle bone by the bending tests (figure 4). In research (Bolte et al, 2000), three-point bending tests were conducted on six adult clavicle bones at an impact rate of 0.5 mm/s. In another work as reported by Untaroiu et al (2009) also, three-point bending tests were conducted on six human post mortem subjects with an impact rate of 1mm/s (quasi-static) and 1 m/s (dynamic). A finite element model was used to compute an elastic modulus as carried out by Rahul et al (2014). For the finite element analysis, the geometry of the clavicle was created from CT/MRI scan data. Figure 5 shows the stress distribution when the load is placed 38 mm from the sterno-clavicular end. The maximum stress occurred on the back side of the clavicle as reported.



**Figure 5: Front and Rear View of Stress Distribution of 135n Load Applied 38 mm from Sterno-Clavicular end (Rahul et al., 2014)**

**Fracture Analysis of Scapula**

Scapula (figure 6) is the large triangular-shaped bone at back of the shoulder. It is attached to the rest of the skeleton through the clavicle at the acromio-clavicular joint. The scapula is held in place by the surrounding muscles. A shallow socket forms at the outer edge of the scapula. The humeral head sits in the shallow socket forming the shoulder joint. Almost 18 different muscles instigate at the scapula and play in six basic movements over the posterior chest wall: elevation, depression, upward rotation, downward rotation, protraction, and retraction. These six movements are restricted by the motion that is permitted in the acromio-clavicular and sterno-clavicular joints as concluded by Gray (1977).

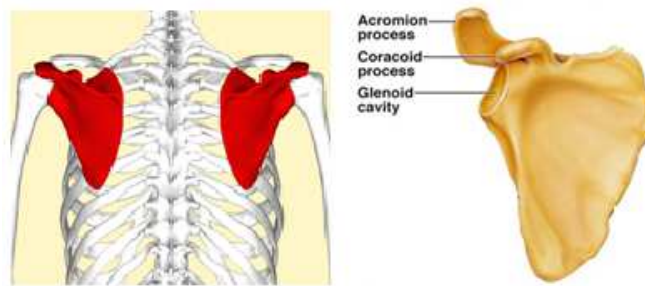


**Figure 6: The scapula**

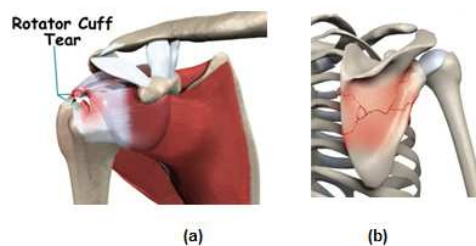


**Figure 7: Rotator Cuff Tear (a) and Scapula Bone Fracture (b)**

Motions of tackling or pitching put great force on the shoulder. The shoulder becomes unstable when its muscles and ligaments are stretched beyond their normal limits. The shoulder separation happens due to tear of ligaments holding the clavicle to the roof of shoulder. Consequently, the clavicle is pushed out of place forming a bump at the top of shoulder. The shoulder separation occurs when arm is stretched to stop topple on a rigid surface. The shoulder separation causes severe pain. The most rotator cuff injuries (figure 7a) happen to middle-aged or older people. As people age and become less active, the rotator cuff tear happens when tendons start to degenerate and lose strength. A tendon is a tough band of fibrous tissue, which is capable of withstanding tension. It connects muscle to bone. Frozen shoulder happens if the shoulder becomes motionless for a period of time. A sudden increase in activity can put immense stress on the shoulders resulting in a loss of flexibility.

Scapula bone fractures (figure 7b) are attributable to 50-60% of all fractures of the shoulder blade. The scapular neck fractures are in charge of 25% of all fractures of the shoulder blade. Over 90% of scapular fractures are simply displaced and they can be overcome with conservative treatment (Gahan et al., 1980). Arthur (2005) was done research on 3D, large-scale, musculo-skeletal model of the upper limb to compare shoulder biomechanics in the case of scapular neck malunion with normal anatomy. It was found that the loss of force in rotator cuff muscles along with other changes in muscle activation, would lead to loss of arm function in patients with scapular neck malunion. Generic and patient-specific finite element models have been used in design of orthopedic implants (Prendergast, 1997) and for predicting the longevity and performance of orthopedic implants (Easley et al., 2007). Resulting from the increased availability of imaging modalities, development of efficient image processing programs, patient-specific FE modeling of the skeletal system has become feasible during the last decade. A number of researchers have investigated different aspects of patient-specific FE modeling for different applications (Basafa et al., 2013; Trabelsi et al., 2011).

The effects of uncertainties in the components of patient-specific models together with bone density, musculoskeletal loads and the parameters of the material mapping relationship on the predicted strain distributions were studied by Gianni et al., (2008). The uncertainty of simulation is a function of the type of movement. Abduction movements present lower uncertainty values than flexion movements. The geometry employed in the FE modeling was produced by segmentation of the scapula from the acquired CT images using Mimics software. The imported geometry was meshed with 4-node linear tetrahedron elements (figure 8a). The percentage of uncertainty in the strain values was considered to be contingent on the number of inaccurate components of the model and the level of uncertainty of individual components. It was also observed that the uncertainty values depend on the type of movement for which musculoskeletal loads are calculated and applied.

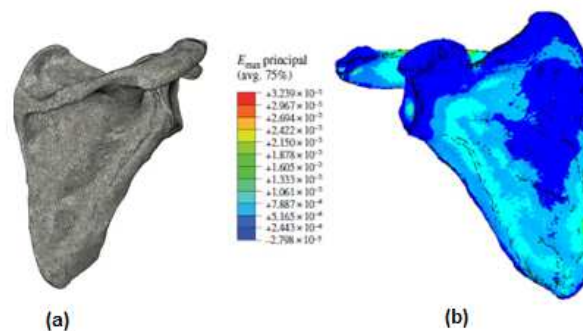


**Figure 8: Finite Modeling of Scapula (a) and Distribution of Maximum Principal Strains (b) (Gianni et al., 2008)**

### Fracture Analysis of Humerus (Upper Arm Bone)

The humerus (figure 9) joins with the scapula at the gleno-humeral joint and connects with the ulna and radius at the elbow joint.

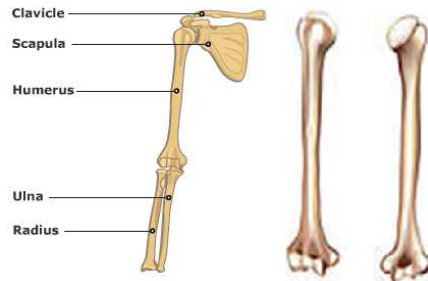


**Figure 9: The Humerus Bone**

Most fractures of the humerus are caused by a direct blow (due to a motor vehicle accident or high-impact fall) to the upper arm. Fractures of humerus bone are of three types: proximal humeral fractures, humeral shaft fractures and distal humeral fractures. Proximal humeral fractures are due to a fall on to an outstretched hand from standing height (figure 10), during seizures or electric shock and a direct blow.

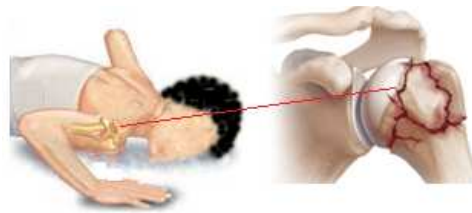


**Figure 10: Proximal Humerus Fracture after fall on Ground**

Humeral shaft fractures (figure 11) result from a direct blow to the upper arm (transverse fractures). Indirect trauma from a fall or a twisting action results in a spiral or oblique fractures (Williams et al., 2010; Shao et al., 2005). The open fractures amount to 2-10%. The distal humerus sits within the cup of the ulna, allowing the ulna to move around it (elbow motion). The elbow joint coordinates movements of the upper extremity, helping the execution of activities of daily living in areas such as hygiene, dressing, and cooking. When the distal humerus is damaged, the function of the elbow joint is impaired. A fracture of the distal humerus occurs when there is a break anywhere within the distal region (lower end) of the humerus. A direct fracture of distal humerus (figure 12) may occur on account of a direct blow. This may occur during a fall (landing directly on the elbow) or by being hit by a hard object (baseball bat, car dashboard or door during a crash). An indirect fracture may take place during a fall if a person lands on his or her outstretched arm with the elbow locked straight. The ulna bone is driven into the distal humerus, causing it to break.



**Figure 11: Humeral Shaft Fractures**

In this paper, proximal humeral fractures are discussed since the upper part of humerus is part of the shoulder joint. Proximal humeral fracture accounts for 10% of all fractures as reported by Baron et al (1996). As age progresses, bone loss within the humeral head may lead to formation of a void in the central bone. For stable osteosynthesis in age-old people, it is necessary to cover voids especially between the humeral centre and the lateral area with supplemental materials (Yamada et al., 2007; Handschin et al., 2008; Matsuda et al 1999) The presence of void concentrates the loads at the screw tips within the medial fracture fragment. The loads were distributed along the entire length of the screws by filling the bone void with calcium triphosphate cement. This reduces peak loads at the screw-bone interface. Finite element models were used to evaluate the effect of void-filling with calcium triphosphate cement on the loads at the end of a proximal humeral fracture osteosynthesis (Feerick et al., 2013). Finite element analysis could enable computation of the effects of void-filling calcium triphosphate cement. When the void was filled with calcium triphosphate cement, the pressure gradient of the bone surrounding the screws in the medial fracture fragment decreased from 21.41 to 0.66 MPa (figure 13).

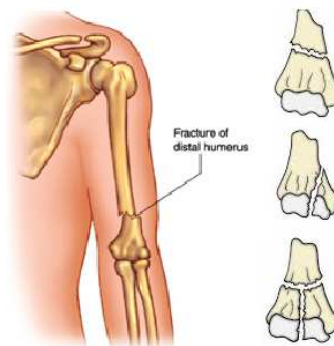


**Figure 12: Distal Humerus Fractures**

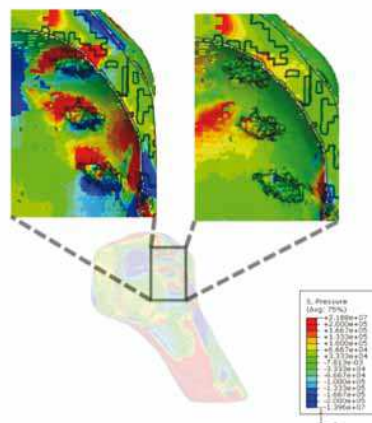


**Figure 13: Pressure Distribution within the Humeral Head (Feerick et al., 2013)**

Finite element analysis was performed by Baumgartner (1976) for the analysis and comparison of existing fixation techniques for proximal humeral fracture reconstruction in hemiarthroplasty. A four-part fracture was also simulated according to a standardized fracture classification. The number of cycles-to-failure was calculated as the migration rate to count the progress of dislocation per loading cycle. Loading of the rotator cuff muscles was simulated by a total tensional load of 40 N. Superior-to-inferior translations of the humeral head centre were detected ranging from -4 to 2.5 mm from 15° to 70° of gleno-humeral abduction. The starting position of the humeral head centre of the first measurement was taken as the reference and simultaneous origin of the coordinate system. The two measured samples showed different characteristics of the curve as seen in figure 14. Stress concentration was shown at two specific regions in the bone-to-implant interface (figure 15).

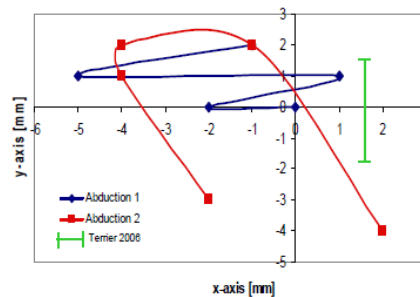


**Figure 14: Translation of the Gleno-Humeral Head Centre**

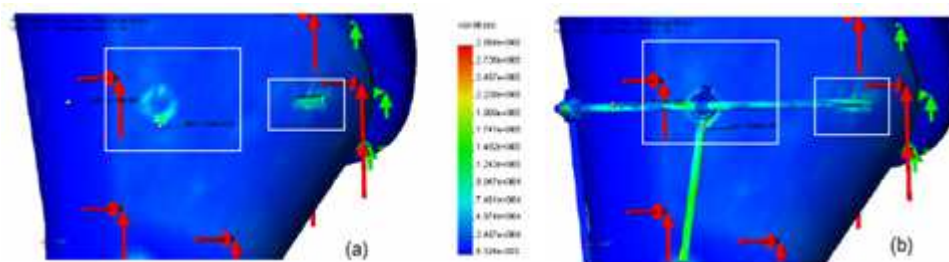


**Figure 15: Local Stresses in Bone-to-Implant Interface (a) without Fixation and (b) with Fixation Displayed (Baumgartner, 1976)**

## SHOULDER JOINTS

The articulations between the bones of the shoulder make up the shoulder joints (figure 16). The joints of the shoulder are the gleno-humeral joint, the acromio-clavicular joint, the sterno-clavicular joint and the scapulothoracic joint.

- The gleno-humeral joint is a ball and socket articulation between the head of the humerus and the glenoid cavity of the scapula,
- The acromio-clavicular (AC) joint where the clavicle meets the acromion of the scapula,
- The sterno-clavicular (SC) joint where the clavicle meets the chest bone (sternum), and
- The scapulothoracic joint where the scapula meets with the ribs at the back of the chest.

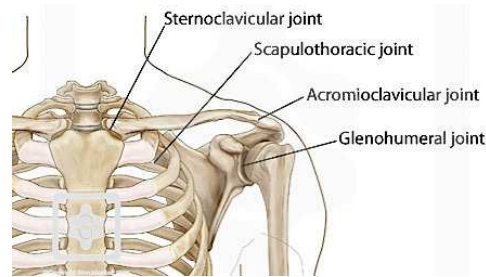


**Figure 16: Shoulder Joints**

### **Gleno-Humeral Joint**

The glenoid forms when the ball head of the humerus fits in with a shallow socket on the scapula. The gleno-humeral joint is a ball-and-socket joint which provides a considerable range of motion and is stabilized by the surrounding tendons, ligaments and muscles. Tendons mainly restrict gleno-humeral translation while the gleno-humeral ligaments limit the rotational movement capacity of the joint.



**Figure 17: The Gleno-Humeral Joint**

The glenoid labrum increases the stability of the gleno-humeral joint by increasing congruency between the glenoid and humeral head and by serving as the attachment for the connective tissues rounding the joint. The glenoid labrum contributes to the depth of the glenoid fossa by 30% to 50% and extends the contact surface area. Thus labrum increases stability by 10% to 20% (Lippitt and Matsen, 1993; Howell and Galinat, 1989; Greis et al, 2002; Fehring et al., 2003). The finite element model was employed to study the tear mechanism in the superior labrum. The finite element model was utilized by Hwang (2014) to evaluate the effect of both superior translation of the humeral head and tension on the long head of the biceps tendon on the strain in the intact labrum. The bones were modeled using rigid quadrilateral shell elements. The cartilages, labrum, and biceps tendon were transformed into hexahedral, solid elements. Solid elements were in addition to the distal end of the biceps tendon to extend the tendon from the site of attachment on the labrum over the head of the humerus and through the bicipital groove (figure 18). The behavior of the labrum tissue with a medium or a large SLAP (superior labral tear from anterior to posterior) tear was different from the small tear or no tear conditions. The predicted von Mises strain on the cross sectional area in the small SLAP tear model is more akin to the intact model than the medium and large tear models. The behavior of the labrum having a slight tear was significantly related to that of intact labrum under all biceps loading conditions (figure 19).



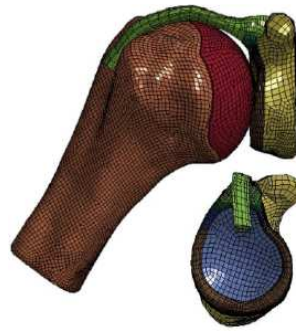


**Figure 18: A Hexahedral Finite Element Model of the Gleno-Humeral Joint, Including the long Head of Biceps Tendon**

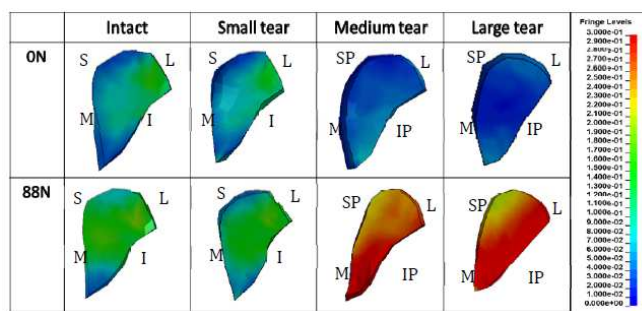


**Figure 19: The Predicted Von-Mises Strain Distribution at the Cross Section of Posterior Edge for the SLAP tear and 0° for Intact Labrum under 0 N and 88 N of Biceps Tension. S, M, I, L, SP, IP Stand for Superior, Medial, Inferior, Lateral, Suproposterior, Inferoposterior, Respectively**

Finite element methods were applied to quantify the contact pressure and its distribution on the healthy cartilage layers for the abduction motion of the gleno-humeral joint (Pujol et al., 2014). From figure 20, it is observed that the scapulo-humeral rhythm where the humerus rotates twice faster than the scapula. In abduction, the humerus describes the trajectory in the scapula plane ( $x_s = 0$ ). The clavicle is rotated less extent than the other bones.



**Figure 20: Abduction. Scapulo-Humeral Rhythm for 00, 300, 600, 900, 1200 and 1500**

**Acromio-Clavicular Joint**

The acromio-clavicular (AC) joint (figure 21) is a junction between the acromion and the clavicle. This joint is comprised of 2 bones (the clavicle and the acromion), 4 ligaments, and a meniscus inside the joint. The normal width of the acromio-clavicular joint is 1-3 mm in younger individuals; it narrows to 0.5 mm or less in individuals older than 60 years. Pediatric acromio-clavicular injuries are caused by the rising popularity of dangerous summer and winter sporting activities. Acromio-clavicular joint injuries are commonly seen after bicycle wrecks, contact sports, and car accidents. Ligaments surround this joint may tear being dependent upon the severity of the injury. Torn ligaments lead to AC joint sprains and separations. Disruption of the AC joint constitutes one of the main causes of scapular malposition and altered scapular

motion that, in turn, may induce a negative influence on rotator cuff function (Gumina et al., 2009; Rockwood et al., 1998). AC joint dislocation results in rupture of the coraco-clavicular (CC) ligaments (Kim et al., 2015). The anatomically aligned SC complex was then scanned with a high-resolution computed tomography scanner into 0.6-mm slices. The finite element model of the SC complex was generated and used for calculating the stress on different parts of the CC ligaments with simulated movements of the scapula. It was noted that the average stress on the conoid ligament during anterior tilt, internal rotation, and scapular protraction was higher, whereas the stress on the trapezoid ligament was more prominent during posterior tilt, external rotation, and retraction.



**Figure 21: The Acromio-Clavicular Joint**

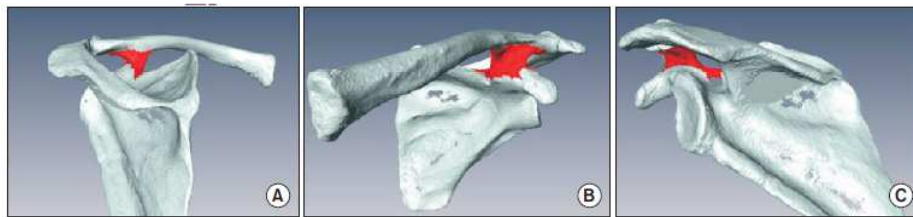


**Figure 22: (A) Posterior View of the Conoid Ligament. (B) Lateral View of the Trapezoid and Conoid Ligaments. (C) Medial View of the Trapezoid Ligament**

**Sterno-Clavicular joint**

The sterno-clavicular joint (figure 23a) is the joint between the sternum and the clavicle. It is structurally classed as a synovial double-plane joint and functionally classed as a diarthrotic joint.

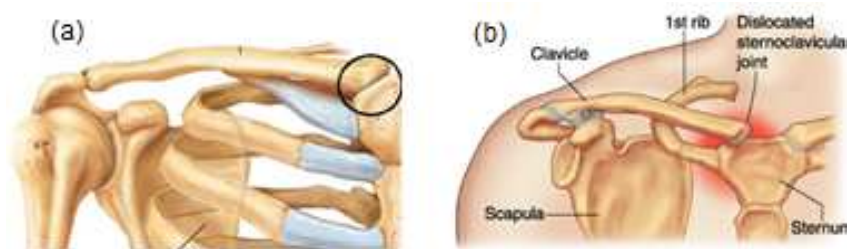


**Figure 23: The Sterno-Zoint (a) and its Dislocation (b)**

The sterno-clavicular joint (figure 23a) is a joint between the sternum and the clavicle. It is structurally classed as a synovial double-plane joint and functionally classed as a diarthrotic joint. Injuries to the sterno-clavicular joint are relatively uncommon, accounting for less than 5% of shoulder girdle injuries. They generally occur in active, adolescent males as a consequence of the high-energy mechanism of injury (figure 23b). Depending on the mechanism of injury (e.g., motor vehicle crash) and the close proximity of the sternum and clavicle to the vital structures of the neck and chest, patients with sterno-clavicular joint injuries may incur severe and life-threatening injuries.

### Scapulothoracic joint

The scapulothoracic joint is not a true synovial joint (figure 24a). This is constituted by the convex surface of the posterior thoracic cage and the concave surface of the anterior scapula. The scapulothoracic articulation allows to increase shoulder elevation. For every 2° of gleno-humeral elevation, there is 1° of scapulothoracic elevation. Scapulothoracic dissociation is the disruption of the scapulothoracic articulation. The mechanism of injury is possibly caused by a blunt force to the shoulder girdle. Scapular winging (figure 24b) is a rare debilitating condition that leads to limited functional activity of the upper extremity. It is the result of traumatic, iatrogenic, and idiopathic processes.

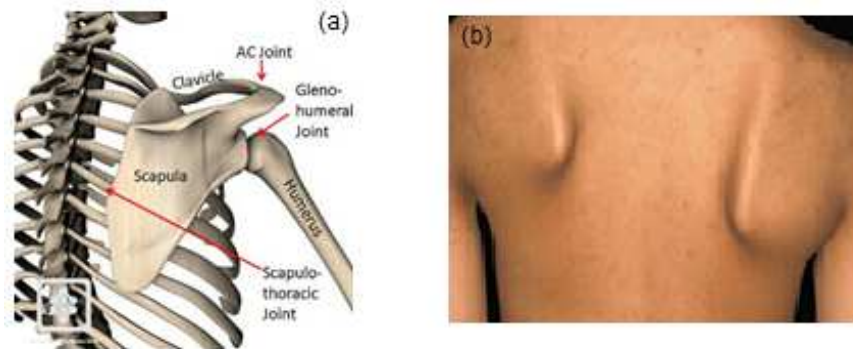


**Figure 24: The Scapulothoracic Joint (a) and Scapular Winging (b)**

Scapulothoracic dissociation is a rare entity that consists of disruption of the scapulothoracic articulation. The mechanism of injury is probably traction caused by a blunt force to the shoulder girdle. Scapular winging (figure 24b) is a rare debilitating condition that leads to limited functional activity of the upper extremity. It is the result of numerous causes, including traumatic, iatrogenic, and idiopathic processes that most often result in nerve injury and paralysis of either the serratus anterior, trapezius, or rhomboid muscles.

### CONCLUSIONS

Shoulder injuries are common vehicle accidents, sports activities fall during walking or running. The clavicle injuries account for 35% to 45% of fractures that occur in the shoulder girdle. The clavicle has been tested experimentally for three-point bending tests and also analyzed using finite element methods to validate its fracture. The shoulder instability is caused owing to motions of tackling or pitching in athletes. The shoulder separation occurs when hand or arm is stretched to stop the fall on a hard surface. As people age and are less active, the rotator cuff tear happens when tendons start to degenerate and lose strength. Frozen shoulder happens if the shoulder becomes motionless for a period of time. Scapula bone fractures are attributable to 50-60% of all fractures of the shoulder blade. Generic and patient-specific finite element models have been applied to design of scapula. Fractures of the humerus are due to a direct blow to the upper arm. Fractures of humerus bone are of three types: Proximal humeral fractures, humeral shaft fractures and distal humeral fractures. As patients age, bone loss within the humeral head may be likely to cause formation of a central bone void. Finite element models were utilized to measure the effect of void-filling in the humeral head. Finite element analysis has been applied to the analysis and comparison of existing and new fixation techniques for proximal humeral heads. The finite element model has been employed to study the tear mechanism in the superior labrum and also the abduction motions of the gleno-humeral joint. Acromio-clavicular joint injuries are often viewed after bicycle wrecks, contact sports, and car accidents. The finite element model has been as well used for calculating the stress on different parts of the ligaments attached to the acromio-

clavicular joint. Injuries to the sterno-clavicular joint are relatively uncommon, being accountable for less than 5% of shoulder girdle injuries. Scapulothoracic dissociation and scapular winging are common problems associated with pseudo scapulothoracic joint.

#### REFERENCES

1. Arthur, V. N. (2005), *The Scapular Neck Fracture: biomechanical, clinical and surgical aspects*, Thesis University Medical Center Utrecht.
2. Baron, J. A., Karagas, M., Barrett, J., Kniffin, W., Malenka, D., Mayor, M. (1996). Basic epidemiology of fractures of the upper and lower limb among Americans over 65 years of age. *Epidemiology*, 7, 612–618.
3. Basafa, E., Armiger, R. S., Kutzer, M. D., Belkoff, S. M., Mears, S. C., Armand, M. (2013). Patient-specific finite element modeling for femoral bone augmentation. *Medical Engineering & Physics Journal*, 35, 860–865.
4. Baumgartner, D. (1976). *Optimisation of Fixation Techniques for Proximal Humeral Fractures*, Thesis, ETH Zurich.
5. Bolte, J., Hines, M., McFadden, J., & Saul, R. (2000). Shoulder Response Characteristics and Injury Due to Lateral Glenohumeral Joint Impacts. *Stapp Car Crash Journal*, 44, 261-280.
6. Easley, S.K., Pal, S., Tomaszewski, P.R, Petrella, A.J., Rullkoetter, P.J, Laz, P.J. (2007). Finite element based probabilistic analysis tool for orthopaedic applications. *Computer Methods and Programs in Biomedicine*. 85, 32–40.
7. Feerick, J.K. E., McGarry, P., Patrick, D. F., Mullett, H. (2013). Effect of calcium triphosphate cement on proximal humeral fracture osteosynthesis: a finite element analysis, *Journal of Orthopaedic Surgery*, 21(2), 167-72.
8. Fehring, E.V., Schmidt, G.R., Boorman, R.S., Churchill, S., Smith, K.L., Norman, A.G., Sidles, J.A., Matsen III, F.A. (2003). The anteroinferior labrum helps center the humeral head on the glenoid. *Journal of Shoulder and Elbow Surgery*, 12, 53-58.
9. Gianni, C., Bart, B., vander, H., Amir, H. W., Zadpoor, A. (2008). Effects of densitometry, material mapping and load estimation uncertainties on the accuracy of patient-specific finite-element models of the scapula, *Journal of the Royal Society Interface*, 17(11), 1666-1672.
10. Gray, H. (1977). *Descriptive and surgical anatomy*. New York: Crown Publishers, 138-144.
11. Greis, P.E., Scuderi, M.G., Mohr, A., Bachus, K.N., Burks, R.T. (2002). Glenohumeral articular contact areas and pressures following labral and osseous injury to the anteroinferior quadrant of the glenoid. *Journal of Shoulder and Elbow Surgery*, 11, 442-451.
12. Gumina, S., Carbone, S., Postacchini, F. (2009). Scapular dyskinesia and SICK scapula syndrome in patients with chronic type III acromioclavicular dislocation. *Arthroscopy*, 25(1), 40-45.
13. Handschin, A. E., Cardell, M., Contaldo, C., Trentz, O., Wanner, G. A. (2008). Functional results of angular-stable plate fixation in displaced proximal humeral fractures. *Injury*, 39, 306–313.
14. Howell, S.M., Galinat, B.J. (1989). The glenoid-labral socket. *Clinical Orthopaedics and Related Research*, 243, 122-125.
15. Hwang, E. (2014). *A finite element model of the superior glenoid labrum*, Kinesiology and Biomedical Engineering, University of Michigan.
16. Kim, Y.S., Kim, I.S., YooI, Y.S., Jang, S.W., Yang, C.J. (2015). An Analysis of Stress Pattern in the Coracoclavicular Ligaments with Scapular Movements: A Cadaveric Study Using Finite Element Model, *Clinics in Shoulder and Elbow*, 18(3).
17. Lippitt, S., Matsen, F. (1993). Mechanisms of glenohumeral joint stability. *Clinical Orthopaedics and Related Research*, 291, 10-28.

18. Matsuda, M., Kiyoshige, Y., Takagi, M., Hamasaki, M. (1999). Intramedullary bone-cement fixation for proximal humeral fracture in elderly patients. A report of 5 cases. *Acta Orthopaedica*, 70, 283–285.
19. Mc Gahan, J. P., Rab, G. T., Dublin, A. (1980). Fractures of the scapulae. *Journal of Trauma*, 20, 880-883.
20. Prendergast, P. (1997). Finite element models in tissue mechanics and orthopaedic implant design. *Clinical Biomechanics Journal*, 12, 343–366.
21. Pujol, F.F., Engelhardt, C.A., Terrier, A., Pioletti, D., Llagunes, J. M.F. (2014). *Musculoskeletal Model of the Glenohumeral Joint: Modeling the contact pressure in the Glenohumeral Joint*, Technical report.
22. Rahul, S., Amar, G., Anand, P. (2014). Finite element analysis of human clavicle bone: A methodology review. *American Journal of Mechanical Engineering and Automation*, 1(5), 54-59.
23. Rockwood, C.A., Williams, G. R., Youg, D.C. (1998). Disorders of the acromioclavicular joint. In: Rockwood CA, Masten FA II, eds. *The shoulder*. Philadelphia: Saunders, 483-553.
24. Shao, Y. C., Harwood, P., Grotz, M. R. (2005). Radial nerve palsy associated with fractures of the shaft of the humerus: a systematic review. *The Bone & Joint Journal, Br.* 87 (12): 1647-1652.
25. Trabelsi, N., Yosibash, Z., Wutte, C., Augat, P., Eberle, S. (2011). Patient-specific finite element analysis of the human femur—a double-blinded biomechanical validation. *Journal of Biomechanics*, 44, 1666–1672.
26. Untaroiu, C. D., Duprey, S., Kerrigan, J., Li, Z., Bose, D., & Crandall, J. R. (2009). Experimental and Computational Investigation of Human Clavicle Response in Anterior-Posterior Bending Loading. *Biomedical Sciences Instrumentation*, 6-11.
27. Williams, G. R., Ramsey, M. L., Wiesel, S. W. (2010). *Operative Techniques in Shoulder and Elbow Surgery*. Lippincott Williams & Wilkins.
28. Yamada, M., Briot, J., Pedrono, A., Sans, N., Mansat, P., Mansat, M. (2007). Age- and gender-related distribution of bone tissue of osteoporotic humeral head using computed tomography. *Journal of Shoulder and Elbow Surgery*, 16, 596–602.

